Supplementary Information

Dual-Phase High-Entropy Ultra-High Temperature Ceramics

Mingde Qin [a], Joshua Gild [a], Chongze Hu [a], Haoren Wang [b], Md Shafkat Bin Hoque [c], Jeffrey L. Braun [c], Tyler J. Harrington [a, b], Patrick E. Hopkins [c, d, e], Kenneth S. Vecchio [a, b], Jian Luo [a, b, *]

[a] *Program of Materials Science and Engineering, University of California, San Diego, La Jolla, CA, 92093, USA*

[b] *Department of NanoEngineering, University of California, San Diego, La Jolla, CA, 92093, USA*

[c] *Department of Mechanical and Aerospace Engineering, University of Virginia, Charlottesville, VA, 22904, USA*

[d] *Department of Materials Science and Engineering, University of Virginia, Charlottesville, VA, 22904, USA*

[e] *Department of Physics, University of Virginia, Charlottesville, VA, 22904, USA*

* Corresponding author. E-mail address: jluo@alum.mit.edu (J. Luo).
Preprint: arXiv:2002.09756

Table S1. Summary of lattice parameters of the corresponding individual metal diborides and carbides. The references are given.

Lattice Parameters *a*, *c* (Å) of the Boride (Metal Diboride)		Lattice Parameter *a* (Å) of the Carbide	
TiB_2	3.031, 3.237 [1]	TiC	4.328 [2]
ZrB_2	3.168, 3.531 [3]	ZrC	4.691 [4]
NbB_2	3.114, 3.265 [5]	NbC	4.454 [6]
HfB_2	3.142, 3.477 [3]	HfC	4.631 [4]
TaB_2	3.097, 3.226 [3]	TaC	4.459 [4]
WB_2	3.022, 3.382 [7]	WC	4.385 [7]

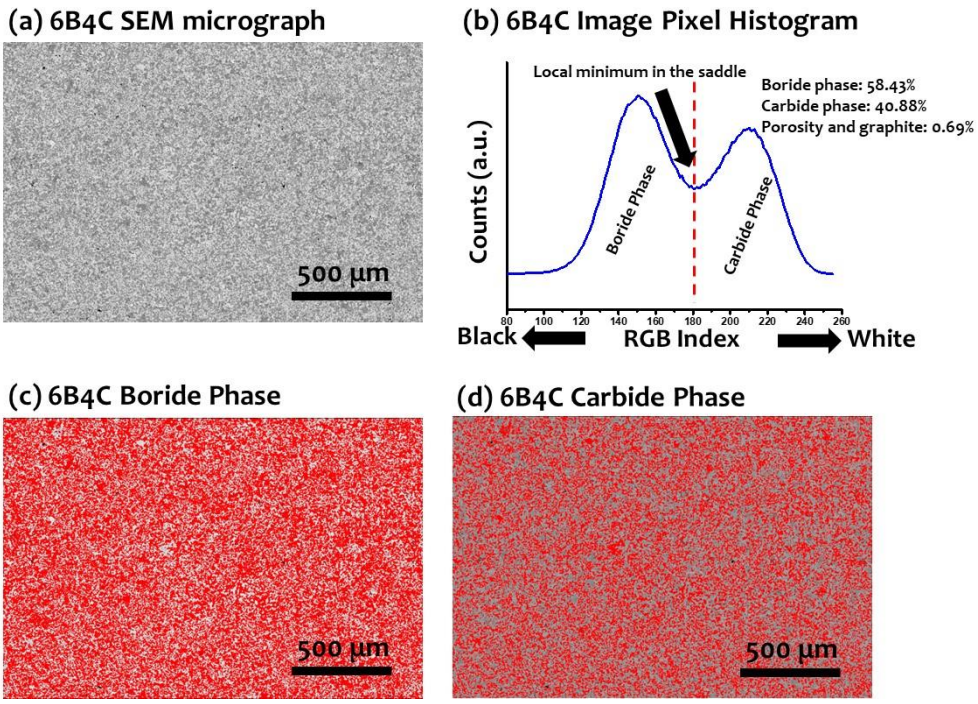

Fig. S1. Evaluation of the volume percentages of the boride (HEB) and carbide (HEC) phases via digital image processing of **(a)** an SEM micrograph. **(b)** The image pixel histogram is obtained via digital image processing, whereas the **(c)** boride (HEB) and **(d)** carbide (HEC) phases are highlighted separately. This example is from a 6B4C specimen.

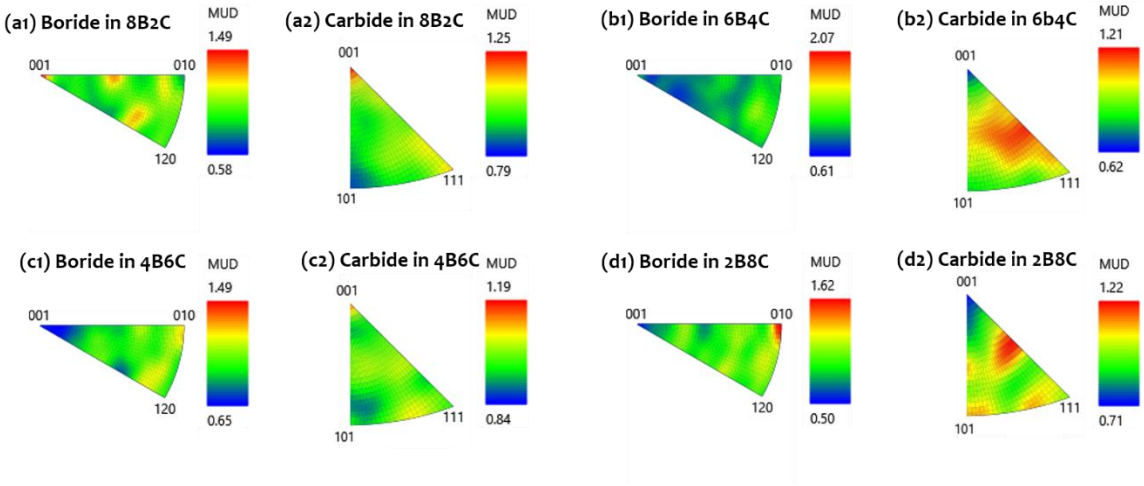

Fig. S2. Inverse pole figures of crystal preferred orientation for Specimens **(a)** 8B2C, **(b)** 6B4C, **(c)** 4B6C, and **(d)** 2B8C, measured from EBSD. Contour maps represent multiples of the uniform distribution (MUD) in each figure. Figures of the boride (HEB) phases are displayed in (a1), (b1), (c1), and (d1), and those of the carbide (HEC) phases are displayed in (a2), (b2), (c2), and (d2).

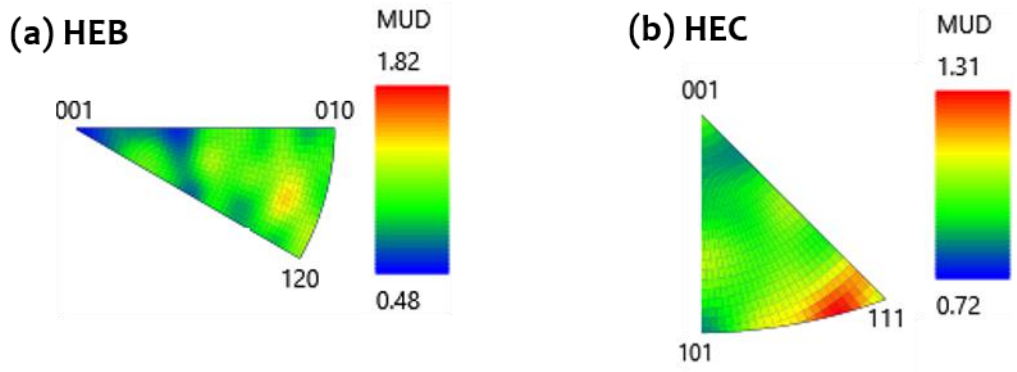

Fig. S3. Inverse pole figures of crystal preferred orientation for Specimens **(a)** HEB and **(b)** HEC, measured from EBSD, where contour maps represent multiples of the uniform distribution (MUD).

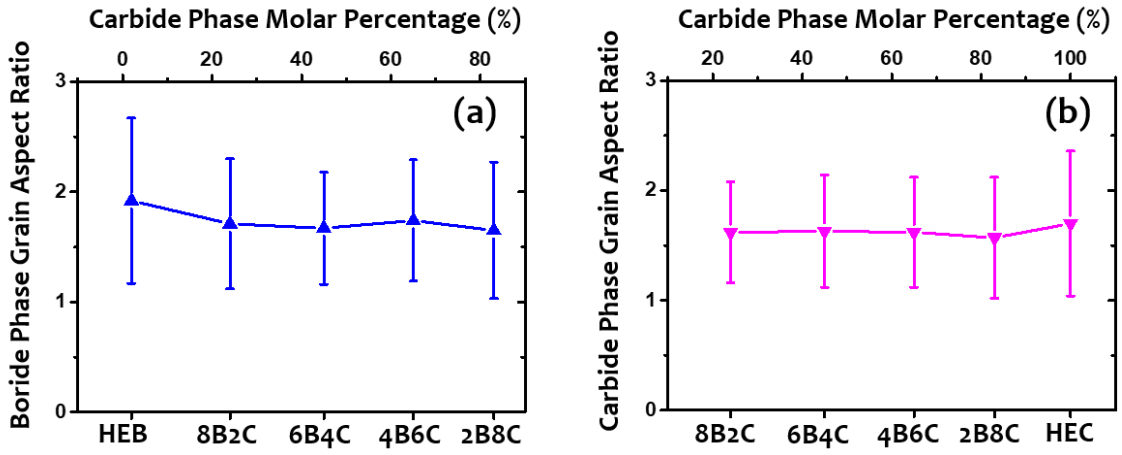

Fig. S4. The grain aspect ratios for **(a)** HEB (boride) phase and **(b)** HEC (carbide) phase, measured from EBSD analysis.

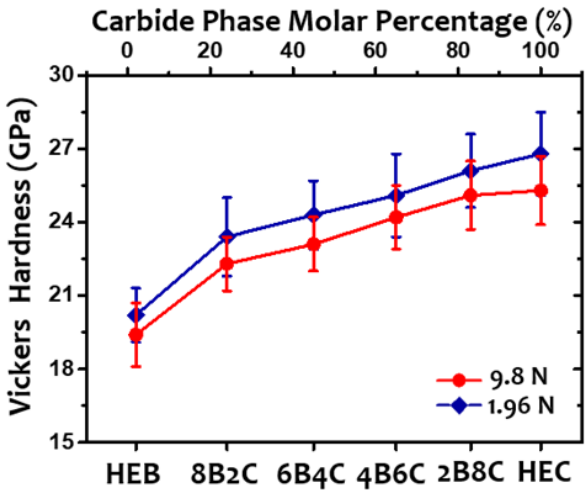

Fig. S5. Measured Vickers' hardness of six specimens (HEB, 8B2C, 6B4C, 4B6C, 2B8C, and HEC) at different indent loading forces of 9.8 N (red circles) and 1.96 N (blue diamonds).

HEB: 98% $(Ti_{0.22}Zr_{0.19}Nb_{0.18}Hf_{0.19}Ta_{0.19}W_{0.03})B_2$ + a minor carbide phase

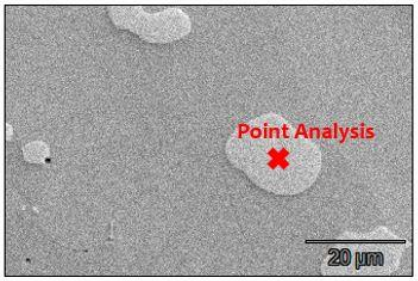

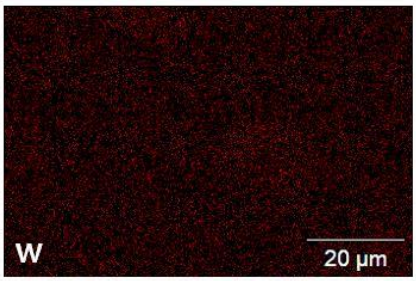

Cations	At. %
Ti	9.2
Zr	18.4
Nb	15.2
Hf	21.8
Ta	32.0
W	3.4

Fig. S6. EDS elemental map of W and a point EDS analysis of the minor carbide phase in the HEB specimen. A relatively large carbide particle is selected for the analysis to ensure the measurement accuracy.

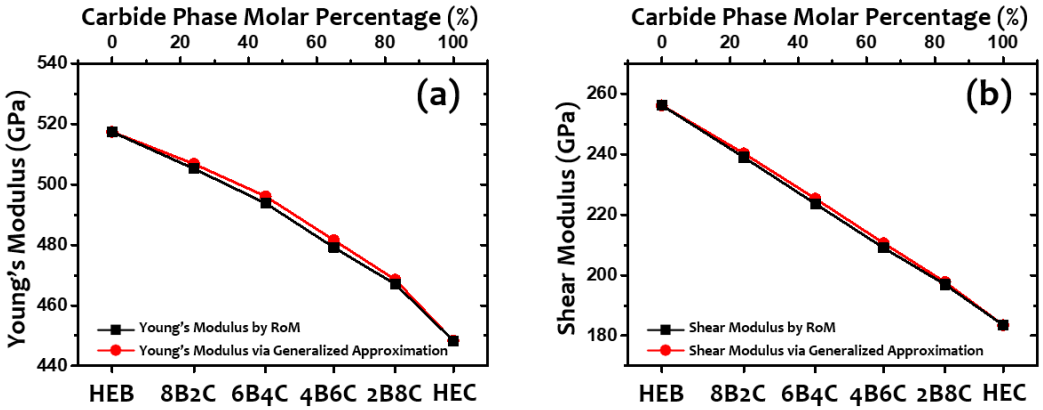

Fig. S7. Comparison of calculated **(a)** elastic moduli and **(b)** shear moduli of six specimens via rule-of-mixture (RoM) (black squares) and the generalized approximation method proposed by Zhang et al. [8] (red circles).

Supplementary References:

[1] Y.-C. Huang, Z.-B. Xiao, Y. Liu, Crystallography of Zr poisoning of Al - Ti - B grain refinement using edge-to-edge matching model, J. Cent. South Univ. (Eng. Ed.) 20(10) (2013) 2635-2642.

[2] Z. Abdullaeva, E. Omurzak, C. Iwamoto, H. Okudera, M. Koinuma, S. Takebe, S. Sulaimankulova, T. Mashimo, High temperature stable WC1−x@C and TiC@C core–shell nanoparticles by pulsed plasma in liquid, RSC Advances 3(2) (2013) 513-519.

[3] B. Lönnberg, Thermal expansion studies on the group IV–VII transition metal diborides, J. Less-Common Met. 141(1) (1988) 145-156.

[4] K. Nakamura, M. Yashima, Crystal structure of NaCl-type transition metal monocarbides MC (M=V, Ti, Nb, Ta, Hf, Zr), a neutron powder diffraction study, Mater. Sci. Eng. B 148(1) (2008) 69-72.

[5] S. Okada, K. Hamano, T. Lundström, I. Higashi, Crystal growth of the new compound Nb2B3, and the borides NbB, Nb5B6, Nb3B4, and NbB2, using the copper-flux method, AIP Conf. Proc. 231(1) (1991) 456-459.

[6] R. Jha, V.P.S. Awana, Vacuum Encapsulated Synthesis of 11.5 K NbC Superconductor, J. Supercond. Novel Magn. 25(5) (2012) 1421-1425.

[7] A. Jain, S.P. Ong, G. Hautier, W. Chen, W.D. Richards, S. Dacek, S. Cholia, D. Gunter, D. Skinner, G. Ceder, K.A. Persson, Commentary: the Materials Project: a materials genome approach to accelerating materials innovation, APL Mater. 1(1) (2013) 011002.

[8] Z.J. Zhang, Y.K. Zhu, P. Zhang, Y.Y. Zhang, W. Pantleon, Z.F. Zhang, Analytic approximations for the elastic moduli of two-phase materials, Phys. Rev. B 95(13) (2017) 134107.